J Mater Sci (2008) 43:2503–2506
DOI 10.1007/s10853-008-2531-3

LETTER

Dislocation-induced crystal rotations in micro-compressed single crystal copper columns

D. Kiener · C. Motz · G. Dehm

Received: 21 January 2008 / Accepted: 6 February 2008 / Published online: 22 February 2008

The flow stress of miniaturized single crystal compression samples fabricated using a focused ion beam (FIB) is known to be size dependent [1–5]. Although sample geometries and loading conditions differ between the individual groups, a general scaling of the flow stress with the sample diameter to a power of about -0.5 ± 0.1 was reported. Nevertheless, there is still no unique model to explain this behavior. Greer and Nix [3] proposed a model of dislocation starvation caused by a lack of multiplication events, Volkert and Lilleodden [4] argued that surface image stresses lead to a loss of dislocations, Zuo and Ngan [6] gave a probability-based criterion for the yield strength of miniaturized compression specimens, while Parthasarathy et al. [7] explained the observed size effect by considering the stochastic of single-ended dislocation sources.

Recent Laue experiments by Maaß et al. [8] demonstrated the existence of strain gradients due to excess dislocations in FIB-fabricated columns. In accordance, micro-structural analysis of FIB-fabricated copper structures by Kiener et al. [9] showed the presence of a dislocation network due to ion bombardment. Whether the dislocations introduced by ion milling are relevant during the micro-compression testing is at the moment unknown. Bei et al. [10] fabricated miniaturized Mo whiskers by a chemical etching method and reported compressive flow stresses in the order of the theoretical strength, in accordance with the data from Brenner [11]. This indicates that the initially present micro-structure and their evolution with ongoing deformation govern the observed size-dependent behavior observed in the micro-compression testing.

In this study, an in situ set-up is applied for the loading experiments to correlate the stress–strain curves to the observed slip steps. Subsequently, the local crystal orientation of the deformed samples is analyzed by electron backscatter diffraction (EBSD) to investigate the micro-structural evolution.

Following the approach of Volkert and Lilleodden [4], single crystal ⟨100⟩ copper specimens were fabricated from a bulk single crystal using an FIB operated at 30 kV and a final milling current of 100 pA. The samples had a circular cross-section, aspect ratios larger 2.5:1, and an unavoidable taper of 3°–5° as in Ref. [4]. This frequently used geometry [3, 4] bears several problems in terms of data evaluation due to the change in sample cross-section and leads to deformation localization at the specimen top. To avoid this variation in cross-section, additionally specimens with square-shaped geometry and thus a homogenous stress over the sample height [5] were fabricated to investigate the local crystal orientation using EBSD. To ensure comparability of the tested micro-structures, the bulk specimen preparation and milling conditions were kept identical to that reported elsewhere [5, 9]. Loading was performed in displacement-controlled open loop at a nominal strain rate of 4×10^{-3} s^{-1} in situ in a scanning electron microscope (SEM) using a micro-indenter (ASMEC UNAT) equipped with a flat tip. The technical stress–strain curves for cylindrical samples with diameters ranging from 0.90 to 6.41 μm are shown in Fig. 1. A clear trend of rising flow

D. Kiener (✉) · C. Motz · G. Dehm
Erich Schmid Institute of Materials Science, Austrian Academy of Sciences, Leoben, Austria
e-mail: daniel.kiener@unileoben.ac.at

D. Kiener
Materials Center Leoben, Forschungs GmbH, Leoben, Austria

G. Dehm
Department of Materials Physics, Montanuniversität Leoben, Leoben, Austria

stress with reduced specimen size is observed. The diameter at half sample height was applied to calculate stresses.

In situ compression tests on ⟨100⟩ specimens with a square cross-section showed that deformation starts at the sample top (Fig. 2a). At a later stage slip continues on a second slip system close to the sample base (Fig. 2b, c). Using the FIB, cross-sections of several deformed columns were prepared with a final milling current of 100 pA and subsequently analyzed by EBSD. Figure 3b shows the misorientation angle map of the deformed copper column shown in Fig. 3a, calculated with respect to the initial crystal orientation. Most of the column remains within 0.5° to the original orientation, which is the accuracy of the EBSD system. The (100) pole figure of the whole sample reveals areas of about 5° misorientation at the edges of the column. This is shown in the two insets at the top right and left of Fig. 3b with the color coding from green to red representing 0° to 5° misorientation from the crystal center to the corners. Note that the corners are tilted in opposite directions.

It is acknowledged that in principle it is possible that FIB damage generates a surplus of dislocations with a certain sign at the column edges, but we have no experimental indication of this. Several publications in the literature report EBSD analysis of FIB-prepared single crystal surfaces [12–14], but no orientation gradient in the undeformed area due to FIB damage was observed. This is

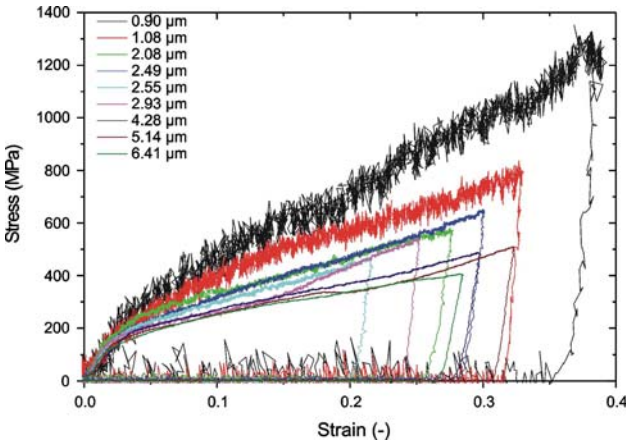

Fig. 1 Technical stress–strain curves for miniaturized ⟨100⟩ oriented single crystal compression samples of diameters ranging from 0.90 to 6.41 µm. A clear trend of rising flow stress with reduced specimen diameter is observed

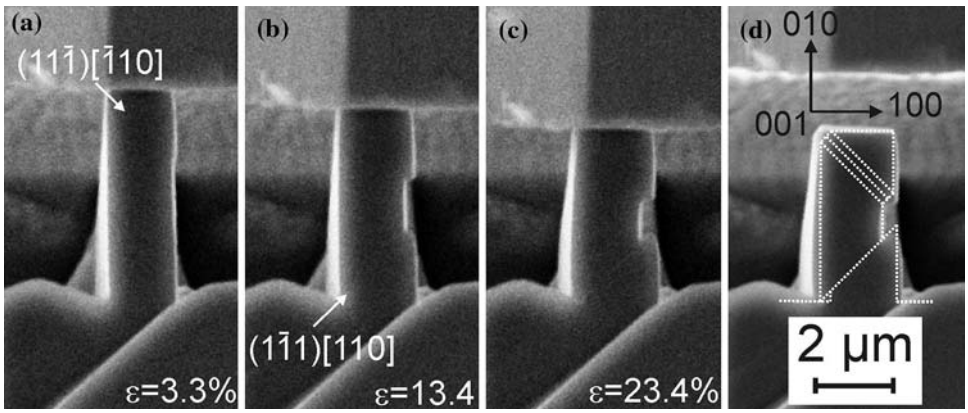

Fig. 2 (**a**)–(**d**) SEM images of a ⟨100⟩ column with a cross-section of 2 × 2 µm taken in situ after (**a**) 3.3%, (**b**) 13.4%, (**c**) 23.4% compression. (**d**) Unloaded specimen with a schematic of the initial crystal orientation and active glide planes during deformation

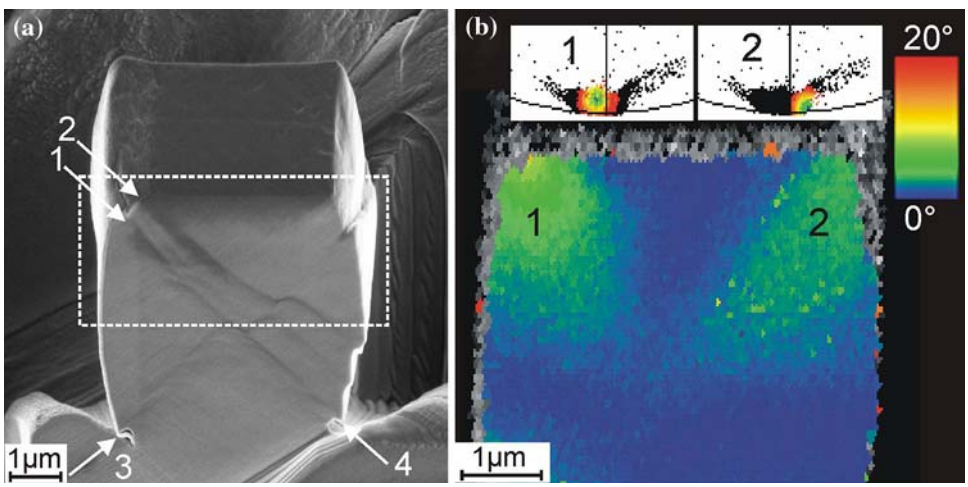

Fig. 3 (**a**) Inclined SEM image of a ⟨100⟩ copper column with a cross-section of 5 × 5 µm after 25% compression. The numbered arrows indicate the acting glide plane and their order of activation as observed during the experiment. (**b**) Color-coded misorientations of the area marked in (**a**) measured by EBSD with a step size of 25 nm on a cross-section of the compressed column prepared by FIB milling

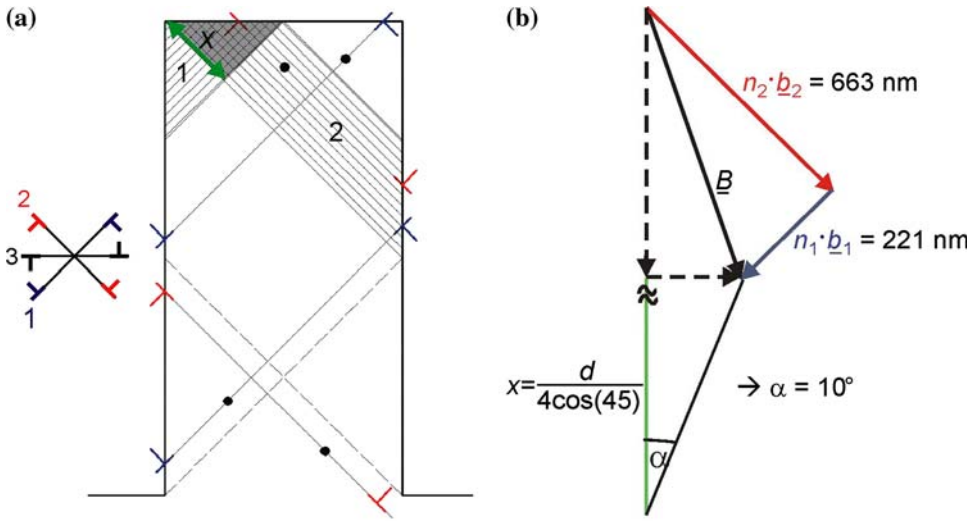

Fig. 4 (**a**) Two-dimensional model with two sets of glide systems (system 1 with n_1 dislocations with Burgers vector $\underline{b}_1$ and system 2 with n_2 dislocations with $\underline{b}_2$). (**b**) Net Burgers vector $\underline{B} = n_1 \cdot \underline{b}_1 + n_2 \cdot \underline{b}_2$ leading to a lattice rotation α in the shaded area (along x in (**a**)). See text for details

also supported by TEM experiments of FIB-damaged single crystal copper [9].

Due to the small aspect ratio of the tested columns, it is likely that dislocations emitted from inside the volume glide to the sample top or bottom as indicated in Fig. 4a for a two-dimensional dislocation model of a ⟨100⟩ copper sample. The flat punch prevents the dislocations from leaving the sample at the top, thus they form pile-ups at the interface, causing the observed local lattice rotations (Fig. 3b). At the bottom of the column the infinite crystal acts as a rigid plate and prevents dislocation escape. The formation of small-angle grain boundaries can be excluded, since the change in orientation is gradual. A quantitative evaluation of this model is outlined below.

Assume dislocation sources of constant density distributed on the glide systems [15] as indicated in the two-dimensional sketch in Fig. 4a: A source located in area 2 can emit dislocations of type 2 into the gray area, while for glide system 1 this can only be achieved by sources located in area 1. Therefore, the probability to observe dislocations of type 2 in the gray area is, according to the area fraction, a factor 3 higher than for dislocations of type 1. Assume the experimental compression of a specimen is accomplished by two sets of slip planes (Fig. 3a), then the net Burgers vector $\underline{B}$ in the shaded area is the sum of n_i dislocations of Burgers vector $\underline{b}_i$ for dislocation system 1 and 2 (Fig. 4), i.e. $\underline{B} = n_1 \cdot \underline{b}_1 + n_2 \cdot \underline{b}_2$. The vertical component of $\underline{B}$ reduces the specimen height, while the horizontal component would shift the loading axis (Fig. 4b). The stiff indenter system is expected to prevent this lateral displacement. However, upon unloading this lateral shift can be often noticed.

Taking x as the average length of the pile-up (Fig. 3b), a local lattice rotation of $\alpha \sim 10°$ is calculated for a compression displacement corresponding to Fig. 3. For symmetry reasons, these dislocation pile-ups are present in each corner near the column/flat punch interface, with equal rotation angle but in opposite directions, as experimentally observed. This rotation angle is an upper limit compared to the experimentally measured misorientations of about 5°, because dislocations will escape during unloading, may annihilate, and/or cross-slip thus reducing the actual misorientation. Additionally, bending stresses evolving during the constrained deformation can activate the horizontal glide system 3, hence reducing the resulting lattice rotations.

The local misorientations observed in deformed micro-compression samples are explained by the formation of dislocation pile-ups at the specimen top due to constrained glide. These pile-ups exert an increasing back-stress on the operating source, thus increasing the stress necessary to nucleate additional dislocations, until the source is deactivated [16], and the deformation is carried on by dislocations emitted from other dislocation sources located close to the bottom of the column (see Fig. 2c, Fig. 3a). This explains the flow characteristics and size dependence reported in micro-compression. In principle this effect could be minimized by increasing the lengths of the columns. This is experimentally limited because of buckling. On the contrary, this experimental constraint can be overcome as shown by recent micro-tensile experiments [17].

Acknowledgements DK thanks the Austrian Fonds zur Förderung der wissenschaftlichen Forschung (Project P17375-N07) and the Austrian Kplus Competence Center Programme (Materials Center Leoben) for financial support. The authors thank Professors O. Kolednik and R. Pippan for valuable discussions.

References

1. Uchic MD, Dimiduk DM, Florando JN, Nix WD (2004) Science 305:986
2. Dimiduk DM, Uchic MD, Parthasarathy TA (2005) Acta Mater 53:4065

3. Greer JR, Nix WD (2006) Phys Rev B 73:1
4. Volkert CA, Lilleodden ET (2006) Phil Mag 86:5567
5. Kiener D, Motz C, Schöberl T, Jenko M, Dehm G (2006) Adv Eng Mater 8:1119
6. Zuo L, Ngan AHW (2006) Phil Mag Lett 86:355
7. Parthasarathy TA, Rao SI, Dimiduk DM, Uchic MD, Trinkle DR (2007) Scripta Mater 56:313
8. Maaß R, Grolimund D, Van Petegem S, Willimann M, Jensen M, Van Swygenhoven H, Lehnert T, Gijs MAM, Volkert CA, Lilleodden ET, Schwaiger R (2006) Appl Phys Lett 89:151905
9. Kiener D, Motz C, Rester M, Dehm G (2007) Mater Sci Eng A 459:262
10. Bei H, Shim S, George EP, Miller MK, Herbert EG, Pharr GM (2007) Scripta Mater 57:397
11. Brenner SS (1957) J Appl Phys 28:1023
12. Rester M, Motz C, Pippan R (2007) Acta Mater 55:6427
13. Kiener D, Pippan R, Motz C, Kreuzer HGM (2006) Acta Mater 54:2801
14. Zaafarani N, Raabe D, Singh RN, Roters F, Zaefferer S (2006) Acta Mater 54:1863
15. Benzerga AA, Shaver NF (2006) Scripta Mater 54:1937
16. Friedman LH, Chrzan DC (1998) Phil Mag A 77:1185
17. Kiener D, Grosinger W, Dehm G, Pippan R (2008) Acta Mater 56:580